

CONF-9605173--17

ANL/ASD/CP--89602

Particle-Beam Profiling Techniques on the APS Storage Ring

B. X. Yang and A. H. Lumpkin

Advanced Photon Source, Argonne National Laboratory, 9700 South Cass Avenue,
Argonne, IL 60439 USA

RECEIVED

NOV 21 1996

OSTI

Abstract. Characterization of the Advanced Photon Source storage ring particle beams includes transverse and longitudinal profile measurements using synchrotron radiation-based techniques. Both optical (OSR) and x-ray synchrotron radiation (XSR) stations are now installed. Spatial resolution of about $\sigma = 55 \mu\text{m}$ was obtained at low current in the visible field initially. This is expected to improve during its commissioning. UV/visible light from the storage ring bending magnet was employed to measure the particle beam with a resolution of $\sigma \sim 80 \mu\text{m}$ and allow operation at 100 mA with the initial x-ray pinhole setup. Early OSR measurements of beam size are consistent with 8.2 nm-rad emittance and 2-3% vertical coupling. Early results with the x-ray pinhole camera are also presented.

INTRODUCTION

The 7-GeV storage ring at the Advanced Photon Source (APS) began commissioning in early 1995. Measurements of the transverse sizes and the bunch length of the stored beam provide important information in characterizing transverse and longitudinal emittance, respectively. Imaging techniques with optical synchrotron radiation were used first due to their simplicity. But OSR spatial resolution is limited mostly due to the diffraction of the synchrotron light beam and depth of the source (Table 1). The optimum resolution is given approximately by $\sigma = (\rho\lambda^2)^{1/3}$ when the full acceptance angle of the imaging system is around $\sigma = (\lambda/\rho)^{1/3}$, where $\rho=39.8$ m is the radius of the particle trajectory.

MASTER

Table 1. The APS Storage Ring Beam Parameter and Optical Imaging Resolution

particle beam natural emittance	8.2 nm-rad	
energy spread	~ 0.1%	
dispersion	92 mm	
vertical coupling	10 %	1 %
rms betatron oscillation (μm)	114 (H) \times 117 (V)	114 (H) \times 37 (V)
total beam size (μm)	146 (H) \times 117 (V)	146 (H) \times 37 (V)
optimal acceptance angle ($\lambda=400$ nm)	3.5 mrad	
optimal resolution	54 μm	

DISTRIBUTION OF THIS DOCUMENT IS UNLIMITED

The submitted manuscript has been authored by a contractor of the U. S. Government under contract No. W-31-109-ENG-38. Accordingly, the U. S. Government retains a nonexclusive, royalty-free license to publish or reproduce the published form of this contribution, or allow others to do so, for U. S. Government purposes.

DISCLAIMER

Portions of this document may be illegible in electronic image products. Images are produced from the best available original document.

DISCLAIMER

This report was prepared as an account of work sponsored by an agency of the United States Government. Neither the United States Government nor any agency thereof, nor any of their employees, makes any warranty, express or implied, or assumes any legal liability or responsibility for the accuracy, completeness, or usefulness of any information, apparatus, product, or process disclosed, or represents that its use would not infringe privately owned rights. Reference herein to any specific commercial product, process, or service by trade name, trademark, manufacturer, or otherwise does not necessarily constitute or imply its endorsement, recommendation, or favoring by the United States Government or any agency thereof. The views and opinions of authors expressed herein do not necessarily state or reflect those of the United States Government or any agency thereof.

It is evident that the resolution of the optical imaging system will not be adequate for the low emittance (low vertical coupling) mode of operation, and imaging with shorter wavelength radiation is needed. In this report we discuss the design and characterization of the APS UV/visible and x-ray pinhole camera beamlines and present initial results obtained from their operation.

UV/VISIBLE BEAMLINE RESULT

The design details of the UV/visible beamline have been reported elsewhere (1,2). Its main challenge is diffraction-limited imaging (angular resolution $\sim 2 \mu\text{rad}$) under high power load. The light transport uses a spherical imaging mirror as the only imaging element to avoid chromatic aberrations. This feature allows convenient alignment and calibration and high transport efficiency which allowed streak and CCD cameras to operate at low beam current. A CCD camera (1/2" format) was placed at the focal point of the mirror to read out the beam image.

Another critical component is the first mirror which, by virtue of high angle reflection, separates the UV/visible radiation from higher energy (x-ray) photons. To achieve $1 \mu\text{rad}$ or less wavefront distortion, the mirror needs to maintain rms flatness to within 60 nm, and the rms temperature difference over the entire mirror surface to less than 1°C . A molybdenum mirror mounted on a water-cooled copper plate was used in the commissioning stage with satisfactory results for stored beam current up to 20 mA. At higher current, we used a water-cooled slotted mirror which allows the high power x-ray beam to pass through and only intercept UV/visible beams at high angles from the orbit plane (2). Unfortunately it distorted slightly under the water/vacuum differential pressure due to a manufacturing defect and could not meet our specifications. An alternative solution, using a tube absorber in front of the pick-up mirror to shield it from the high-power x-ray beam, is currently under development.

Due to its limited spatial resolution, our OSR station is mainly used for streak camera measurements of beam bunch length and longitudinal dynamics since the setup of the x-ray pinhole camera. Figure 1 shows a typical dual sweep streak camera image taken with the Mo-mirror at low current (7 mA single bunch). The vertical scan is driven by a synchroscan unit operating at 117.3 MHz. Since the frequency is one-third of that of the storage ring rf frequency, the streak camera acquires the bunch data every three buckets. Figure 2 shows dual sweep images with different horizontal time scale and signatures of phase oscillations at 40 kHz and 360 Hz, which are likely due to output ripples of the rf power amplifier power supply. The amplitude of these signatures is checked periodically such that any abnormal conditions of the rf system should be spotted early.

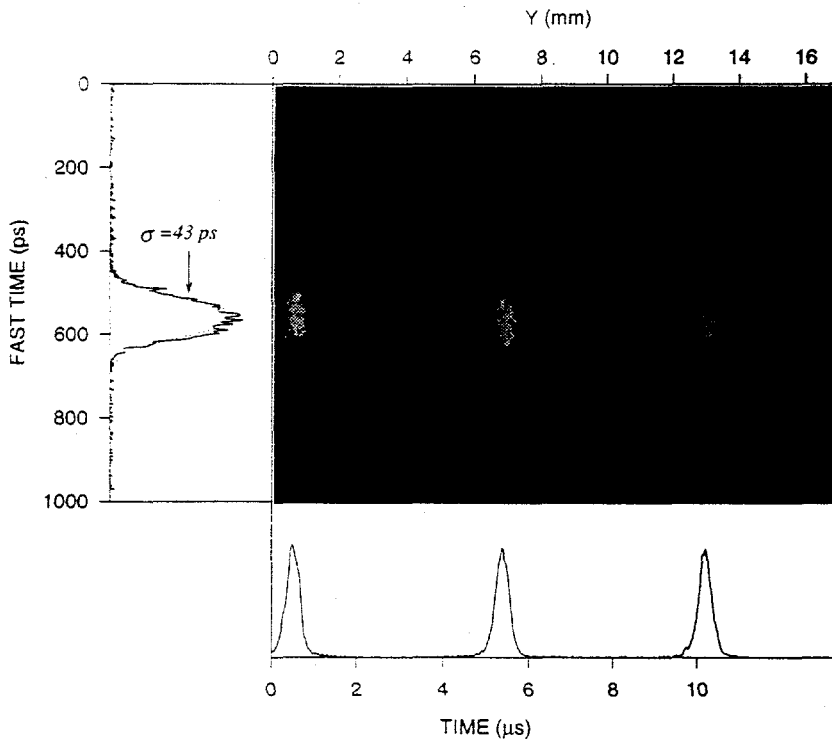


Figure 1 A typical dual-sweep streak camera image, a side view of the beam bunch with the fast-time axis in the vertical direction, and slow-time in the horizontal. In setting up this experiment, the beam image was rotated 90 degrees. Hence the horizontal width of the image actually shows the vertical size of the beam (top scale), while the vertical dimension of each bunch image shows the beam length in time ($\sigma \sim 45$ ps). To read the time between passes, the lower horizontal scale should be used.



Figure 2A A dual-sweep streak camera image of a single bunch. The full vertical scale is 0.96 ns and the full horizontal scale 200 μ s. The bunch exhibits a 40-kHz phase oscillation with a peak-to-peak amplitude of about 80 ps. The stored beam is 4.9 mA.



Figure 2B A dual-sweep streak camera image of a single bunch. The full vertical scale is 0.96 ns and the full horizontal scale 20 ns. The bunch exhibits a 360-Hz phase oscillation with a peak-to-peak amplitude of about 30 ps. The stored beam is 4.9 mA.

Figure 3 shows the dependence of bunch length on the single-bunch current. In the run dated 8-19-95, a significant bunch lengthening (slope change) was observed before the maximum bucket charge was reached, indicating the onset of a longitudinal instability at high bunch current. It can also be seen that the measured values are well within the APS design goal of a 100-ps bunch length at 5-mA single bunch current.

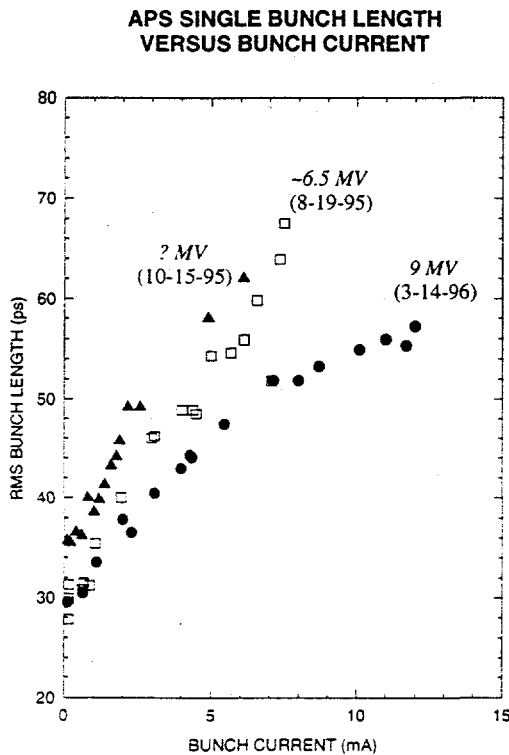


Figure 3 Single-bunch current versus bunch length for different rf gap voltages.

X-RAY PINHOLE BEAMLINE

The initial setup of the pinhole camera is entirely inside the storage ring tunnel and is shown in Fig. 4. It is similar to those used elsewhere (3,4). The design parameters are given in Table 2. The magnification of the pinhole camera is

$$M = \frac{\text{detector - pinhole distance}}{\text{source - pinhole distance}} = 0.442 .$$

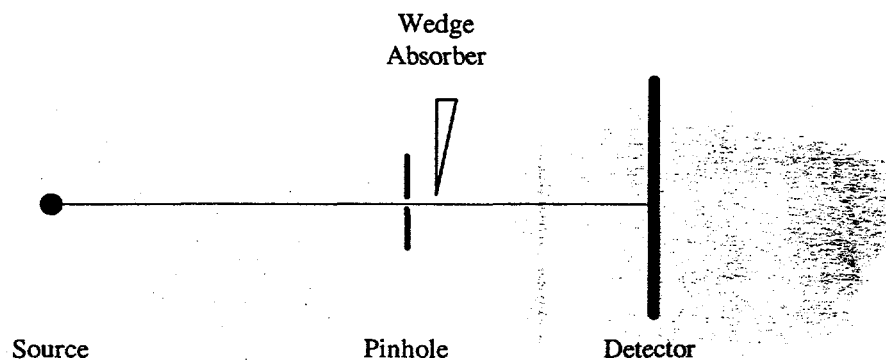


Figure 4 Experimental setup of the x-ray pinhole camera.

Table 2. Design Parameter of the Pinhole Camera (in-tunnel setup)

Component	Location (from source)	Comments
Aluminum windows	13.30 m	2 mm (H) × 12 mm (V), water-cooled, two windows and a pumping station interlocked with the photon shutter are used for vacuum safety
Pinhole	13.35 m	25 μm × 25 μm square aperture, formed with two sets of perpendicular tungsten blades 1 mm thick
S/S wedge	13.50 m	stainless wedge, adjustable attenuator (0 to 10 mm thick)
Scintillator	19.26 m	10 mm × 10 mm CdWO ₄ crystal mounted on a grid; light is collected from the back side of the crystal
Read-out optics/camera	19.26 m	a telemicroscope (Questar SZ-FR1) with a ½" CCD camera, resolution(1-σ) = 8 μm at the scintillator, 18 μm at the bending magnet source

A typical pinhole image is shown in Fig. 5. The beam profile fits well with Gaussian form and the profile widths are 157 μm horizontally and 115 μm vertically. These values are consistent with the design goal of the APS storage ring with 8.2 nm-rad emittance and 10% vertical coupling. However while the horizontal width is the same as measured with OSR imaging, the vertical size is significantly higher than that measured with OSR or with an x-ray pinhole camera with higher magnification (4).

It is likely that the point spread function of the scintillation detector dominates the total resolution due to the low magnification in the present setup.

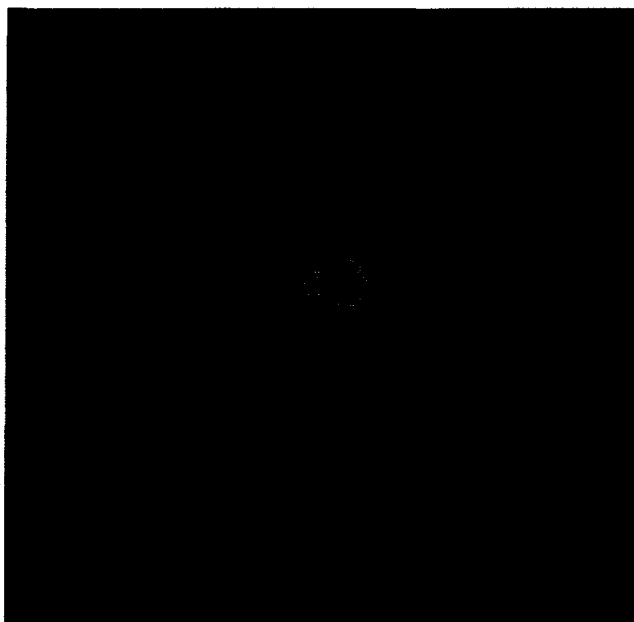


Figure 5. X-ray pinhole image of stored beam in the APS storage ring (100 mA @ 7 GeV, May 6, 1996). The camera field of view is 2.7 mm \times 2.7 mm, and the rms beam size is 157 μ m horizontally and 115 μ m vertically.

One significant advantage of the x-ray pinhole camera over the UV/visible imaging is the stability of its image, since the latter is susceptible to mirror vibrations in the long transport line. This feature can be used to measure the dispersion function at the source point. Figure 6 shows a set of beam profiles taken with slightly different rf frequencies, or different beam energies. From the displacement of beam centroid, we deduce the dispersion at the source to be 74 μ m per 0.1% $\Delta E/E$. This value can be compared with the calculated value of 92 μ m per 0.1% $\Delta E/E$ at the design lattice.

SUMMARY

Optical and x-ray synchrotron radiation imaging techniques have been used to characterize the Advanced Photon Source storage ring particle beams. The longitudinal measurement shows that the bunch length is within the design specifications of 100 ps, and the x-ray pinhole measurement shows that the transverse beam size is consistent with the design emittance of 8.2 nm-rad and less than 10% vertical coupling. The dispersion function at the bending magnet source point has also been measured to be 74 μ m per 0.1% $\Delta E/E$, less than the design value of 92 μ m per 0.1% $\Delta E/E$.

The resolution of our current x-ray pinhole setup is not sufficient for measuring the APS storage ring beam at vertical couplings lower than 10%.

Design and construction of a beamline with higher magnification and resolution is in progress, which will improve the resolution for characterizing low emittance beam.

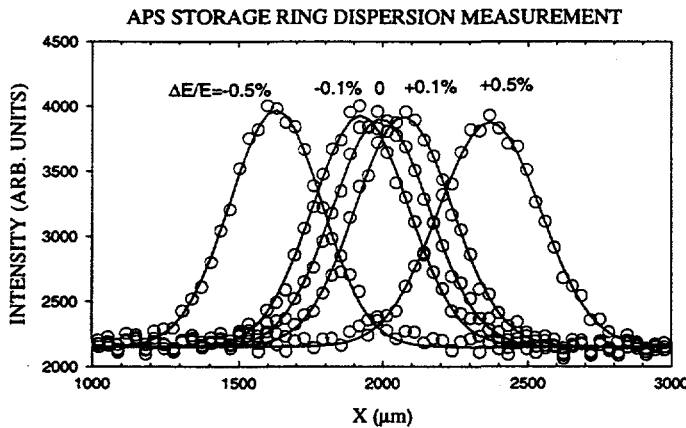
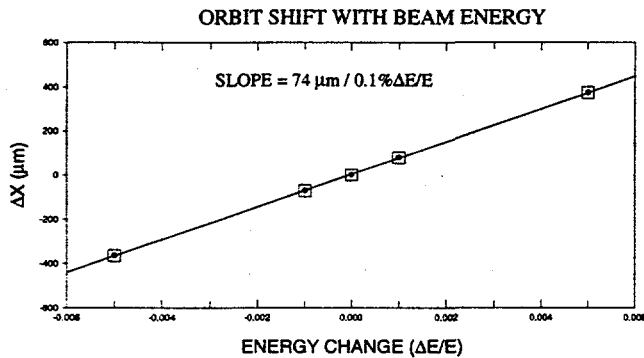


Figure 6. Top: horizontal beam profiles at different beam energies. Bottom: the horizontal coordinates of the beam centroid as a function of beam energy change.



REFERENCES

1. Yang, B. X., and Lumpkin, A. H., "The Planned Photon Diagnostics Beamlines at the Advanced Photon Source," Beam Instrumentation Workshop 1994, AIP Conference Proceedings 333, (AIP, New York, 1995) pp. 252-258.
2. Yang, B. X., and Lumpkin, A. H., "Initial Time-Resolved Particle Beam Profile Measurements at the Advanced Photon Source," Proceedings of Synchrotron Radiation Instrumentation 1995, Rev. Sci. Instr. (to be published).
3. Elleaume, P., Fortgang, C., Penel, C., and Tarazona, E., "Measuring Ultra Small Electron Emittance Using an X-Ray Pinhole Camera," ESRF/MACH ID 95/25, 1995.
4. Cai, Z., Yun, W., Lai, B., Gluskin, E., and Legnini, D., "Beam Size Measurement of the Stored Electron Beam at the APS Storage Ring Using Pinhole Optics," Proceedings of Synchrotron Radiation Instrumentation 1995, Rev. Sci. Instr. (to be published).